Wafer-Scale Transfer-Free Graphene MEMS Condenser Microphones

Pezone, Roberto; Baglioni, Gabriele; Di Paola , Leonardo ; Sarro, Pasqualina M.; Steeneken, Peter G.; Vollebregt, Sten

Publication date
2023

Document Version
Final published version

Published in
Proceedings of the 2023 22nd International Conference on Solid-State Sensors, Actuators and Microsystems (Transducers)

Citation (APA)
Pezone, R., Baglioni, G., Di Paola , L., Sarro, P. M., Steeneken, P. G., & Vollebregt, S. (2023). Wafer-Scale Transfer-Free Graphene MEMS Condenser Microphones. In *Proceedings of the 2023 22nd International Conference on Solid-State Sensors, Actuators and Microsystems (Transducers)* (pp. 362-365). IEEE.

WAFER-SCALE TRANSFER-FREE GRAPHENE MEMS CONDENSER MICROPHONES

Roberto Pezone[1], Gabriele Baglioni[2], Leonardo di Paola[1], Pasqualina M. Sarro[1], Peter G. Steeneken[2,3], and Sten Vollebregt[1]

[1]Laboratory of Electronic Components, Technology and Materials (ECTM), Department of Microelectronics, Delft University of Technology, The Netherlands

[2]Kavli Institute of Nanoscience, Department of Quantum Nanoscience, Delft University of Technology, The Netherlands

[3]Department of Precision and Microsystems Engineering (PME), Delft University of Technology, The Netherlands

ABSTRACT

This paper outlines the first transfer-free multi-layer (ML-gr) graphene-based MEMS condenser microphone with a high aspect-ratio suitable for sensitive miniaturized portable microphones. This fabrication flow avoids thick polymers needed to realize suspended graphene-polymer heterostructures over air cavities, which generally limit the response by introducing higher mass and stiffness. Several devices are characterized both mechanically and electrically, showing pull-in voltages up to 9.5 V and resonance frequency limited bandwidths of up to 127 kHz. The work paves the way to realize next-generation graphene microphones with a 4.5x area reduction compared to current state-of-the-art MEMS microphones.

KEYWORDS

Microphones, MEMS, graphene, membranes, wafer-scale, resonators.

INTRODUCTION

Large and highly-compliant diaphragms suspended over thin gaps are needed to increase microphone performance [1]. Several works highlighted the potential of graphene as the movable electrode for condenser microphones due to its high flexibility and ability to conduct electrical current [2-9]. The movable electrode presents a significant limitation in targeting higher compliant areas, especially for compact micromachined MEMS solutions. Moreover, even though the thinnest suspended graphene has been obtained with transfer-based methods, the device performance is still lower than commercial MEMS-microphones due to the limited sensitive area possible with the transfer, which is related to the challenge of transferring graphene layers over large cavities [2]. Given this limit, hundreds of nm-thick graphene/polymer stacks were suspended with diameters of up to 3.5 mm over cavities [5]. However, this approach does not align with the miniaturization trend where the state-of-the-art MEMS microphones have diameters ranging between 0.6 – 1 mm. In addition, the polymer mass support decreases the resonance frequency in the audible range [5]. Last but not least, none of the previous works are fabricated in a wafer-scale approach that might be compatible with ASIC integration and high-volume manufacturing in a System-In-Package (SiP) or System-On-Chip (SoC) technology. We demonstrate the first 7-nm thick ML-gr based MEMS condenser microphone with a wafer-scale and transfer-free method based on a full dry release by bulk micromachining and vapor HF (VHF) etch.

EXPERIMENTAL SECTION

Process-flow

A 100 mm silicon p-type wafer is thermally oxidized at 1000 °C, forming 1μm SiO_2 as an insulating layer for the future back-plate and as landing layer for the final bulk silicon etching. A layer of 100 nm LPCVD SiN_x is deposited at 850 °C and patterned in correspondence with the venting holes of the suspended back-plate (Fig. 1(a)). LPCVD is also used to deposit 1 μm of Poly-Si (SiH_4 45 sccm) at 605 °C with consequent Boron doping with 45 keV, and 10^{15} at/cm^2. After the annealing and doping activation step of 1 h at 950 °C in N_2/Ar atmosphere, the continuous Poly-Si layer is patterned to define the back-plate area with Cl/HBr chemistry (Fig. 1(b)). Then, as a future sacrificial layer, a PECVD TEOS film of 5 μm is deposited and annealed at 1000 °C in Ar/N_2 environment. A second film of LPCVD SiN_x (100 nm), adopted as the capping and clamping area for the final sacrificial oxide etching is deposited (Fig. 1(c)) and etched accordingly to the future graphene suspended area and vias for the counter electrode contacts (Fig. 1(d)). A PECVD TEOS film of 5 μm is deposited on the back side and patterned to work as an etching mask for the DRIE (Deep Reactive Ion Etching) process. A thin film of 50 nm Mo to serve as catalyst for the graphene CVD is sputtered at 50 °C and etched by dry etching with Cl/O_2 chemistry (Fig. 1(e)). Graphene is then synthesized at 935 °C with an in-house reactor AIXTRON Black Magic Pro at a pressure of 25 mbar with H_2 as a reducing agent for the oxidized Mo and a CH_4 step for the growth (Fig. 1(f)). Next, Cr/Au (20/200 nm) are evaporated by electron-beam evaporation and patterned using a lift-off technique with Acetone at 40 °C, IPA, and DI-water (Fig. 1(g)). Mo is wet-etched in H_2O_2 and subsequently washed in DI-water. DRIE is performed on the back-side, and the SiO_2 (1 μm) is we-etched in BOE 1:7 chemistry (Fig. 1(h)). A final DRIE through the back-side is performed to completely etch the exposed Poly-Si in correspondence with the venting holes using the SiN_x layer as an etching mask (Fig. 1(i)). After dicing of the 1 cm x 1 cm chips, the VHF (Vapor HF) etch is performed at 45 °C with 100% anhydrous HF, N_2, EtOH in a commercially available Primaxx μEtch system at 125 Torr (Fig. 1(l)).

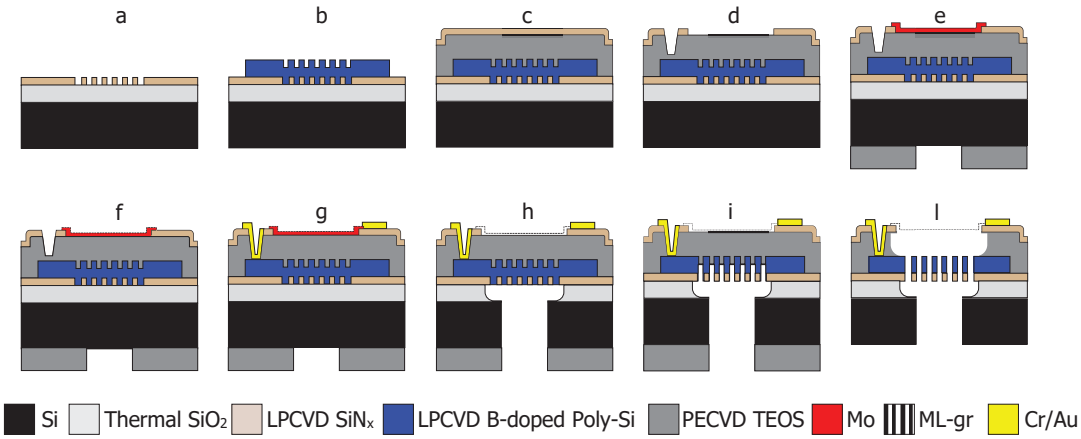

Figure 1: Fabrication process flow. (a)Thermal SiO_2 (1 µm), dry-etching of LPCVD SiN_x (100 nm). (b) LPCVD Poly-Si (1 µm) patterning by dry-etching. (c) PECVD TEOS (5 µm) and LPCVD SiN_x. (d) Combined wet/dry etching of TEOS for tapered sidewalls contact opening. (e) Mo (50 nm) sputtering and dry-etching, PECVD TEOS (5 µm) etch mask for DRIE (f) Chemical Vapor Deposition at 935 °C and 25 mbar with CH_4/H_2. (g) Wet-etching of residual TEOS on Poly-Si, Cr/Au (20/200 nm) lift-off. (h) Mo etching by H_2O_2. (h, i, l) DRIE of Si, wet-etching of SiO_2 landing layer, DRIE of 1 µm of Poly-si using pre-patterned SiN_x as hard mask, TEOS VHF release etch of graphene membrane.

Characterization methods

A Horiba HR800 Raman spectrometer equipped with a 514.4 nm Ar+ laser, 100x objective with a NA of 0.9, is used for the crystallinity characterization of the multi-layer graphene. An atomic force microscope (AFM) from Cypher Asylum Research is operated in air topography mode to determine the multi-layer graphene thickness. A Scanning Electron Microscope (SEM) Hitachi Regulus 8230 is used to verify the fully suspended structure. A Polytec MSA-400 and OFV534 are used to determine the f_{01} by piezoelectric actuation at low pressure. Electrical measurements as C_0 and $V_{pull\text{-}in}$ are performed with a Cascade Summit probe station connected to an Agilent 4294A Precision Impedance Analyzer.

RESULTS AND DISCUSSION

The fabricated devices are classified into three geometries: trampoline membranes with 2R = 320 µm, 220 µm (geom. A, C), and a fully clamped membrane with 220 µm (geom. B). The gap of 5 µm is chosen for all device geometries as they are processed in the same wafer. SEM images of a trampoline device 2R = 220 µm (geom. C) before and after the vapor HF are shown in Fig. 2. In Fig. 3a, a Raman Spectroscopy of a suspended membrane (complete process) describes the low invasiveness of the suggested process flow. A graphene defectivity of $I_D/I_G \sim 0.2 \pm 0.03$ is reported, and the ω_D, ω_G, and ω_{2D} are centered in 1348.1, 1572.2, and 2682.5 cm^{-1} with standard deviations of 4.1, 3.5, and 5.3. Also, based on $I_{2D}/I_G \sim 0.89 \pm 0.25$, these data are typical for multi-layer graphene, and considering the FWHM 2D, it can be characterized as turbostratic graphene where the stacked layers are more twisted with respect to each other [10]. Atomic Force Microscope measures a graphene mean-thickness of ~7 nm, accordingly to previous work [9] (Fig. 3b). The base capacitance C_0 is measured with 100 mV at 100 kHz for more than 50 devices before the final vapor HF release. The results are in line with the analytical model for a parallel plate capacitor in Eq. 1 within < 15 % deviation. This confirms the fabrication success before the release. Any influence of the fringes and venting holes are not considered for simplicity.

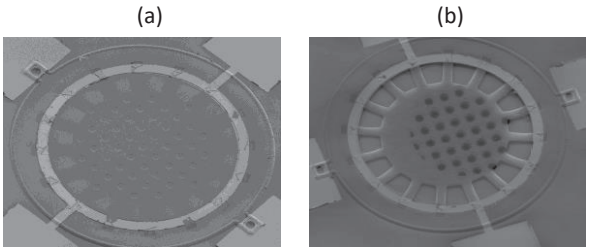

Figure 2: SEM images of suspended 220 µm ML-gr (a) before and (b) after the release.

$$C_0 = \frac{\varepsilon_0 \varepsilon_{TEOS} A}{gap} \quad (1)$$

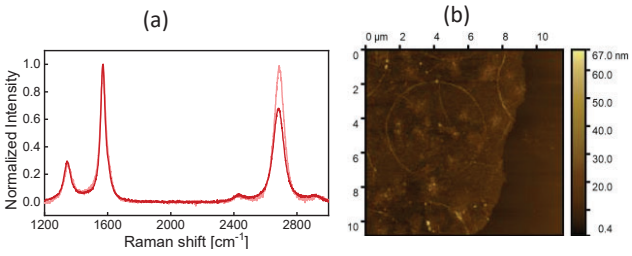

Figure 3: (a) Raman specotroscopy characterization of suspended region after VHF. (b)Thickness of the multi-layer graphene grown in the same substrate where final devices are fabricated. Measurement results and procedure are aligned with previous works [9]. The thickest parts are related to large foldings in correspondence of the circular edges and polymer residuals. The circles are related to imprint left from the the Mo seed layer that is grown in a pre-patterned region.

After the final vapor HF, the successfully released devices show lower C_0, which is due to TEOS removal. In Fig. 4, a V_{AC} between 100 mV – 1V at 100 kHz is forced to the capacitor electrodes to verify the success of the membrane release. A linear increment of C_0 due to the increase of the V_{AC} amplitude aligns with the higher membrane oscillation magnitude. A $\Delta C_0 \approx 1.2$ fF is measured with an expected membrane dynamic displacement of ≈ 150 nm based on Eq. 1. Imposing a voltage offset ($V_{bias} > 0$), the C_0 shows a non-linear relation due to the electrostatic forces introduced by the constant voltage (Eq. 2).

$$\vec{F} = -\frac{{V_{bias}}^2}{2}\frac{\partial C}{\partial x}\overrightarrow{u_x} \qquad (2)$$

None of these responses are found for the devices before release, i.e. where VHF has not been performed. In this case, as expected, the C_0 stays constant despite the different electrical stimulations. Since a condenser microphone needs $V_{bias} \neq 0$ V to keep the capacitor plates at a constant charge, a V_{bias} window of -9.5 V – 9.5 V is forced to both electrodes to investigate the $V_{pull\text{-}in}$. At $V_{pull\text{-}in}$ (Eq. 3), the movable plate starts to become unstable due to the total amount of charges that is large enough to overcome the spring restoring force. This point corresponds to a membrane position that is at 1/3 of the gap [11]. If the voltage is further increased, the two plates can remain stuck together as long as the charges remain in place.

$$V_{pull-in} = \sqrt{\frac{8kgap^3}{27\varepsilon_0 A}} \qquad (3)$$

In Fig. 5a, the C_0-V_{bias} curves define the operational voltages of all inspected devices, where outside those electrode. The $V_{pull\text{-}in}$ is found to be between 2 – 9.5 V for all inspected devices. The differences are related to the membrane clamping, where for a fully clamped geometry, the highest $V_{pull\text{-}in}$ is found. The reason could be attributed to the lower mechanical stiffness related to the tethers of the trampoline geometries (geom. A, C) compared to the case where the membrane is fully clamped (geom. B). Previous work also found lower stiffness for similar types

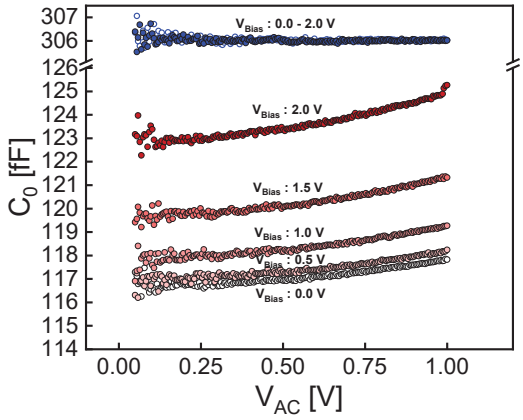

Figure 4: C_0 comparison of two devices with same geometry (2R = 220 µm, trampoline) before (blue points) and after the VHF release (red points).

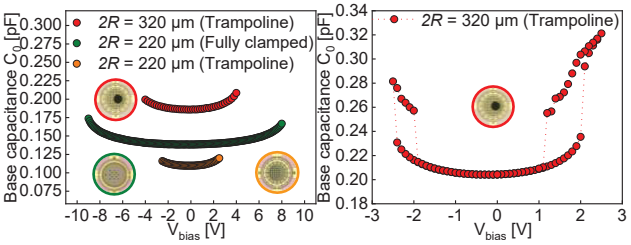

Figure 5: (a) C_0-V_{bias} measurements by Keysight 4294A Impedence Analyzer with V_{AC} 100 mV, 100 kHz. The capacitance-voltage relation (C_0-V_{bias}). Different sizes, graphene clamping and electrodes geometries are also inspected (insight pictures). $V_{pull\text{-}in}$ occurs at the V_{bias} endpoints. (b) Example of $V_{pull\text{-}in}$, $V_{pull\text{-}out}$ of 2R=320 µm device.

of devices, when comparing both geometries [9]. An example of cyclic actuation to determine the $V_{pull\text{-}in}$ and $V_{pull\text{-}out}$ of a 2R = 320 µm device is shown in Fig. 5b. In this case, at $V > V_{pull\text{-}in}$, the membrane starts to collapse on the counter electrode with a limited area due to a non-uniform electrostatic force distribution. This disuniformity is related to the back-side misalignment where some venting holes are not opened (Fig. 2b). In correspondence of this limited area, in the case of a trampoline with 2R = 320 µm, once the membrane collapses, a $\Delta C_0 \approx 80$ fF is measured (Fig. 5b) instead of $\Delta C \approx 400$ fF. We found that with only a $V_{bias} > 8$ V, the membrane entirely collapses on the counter electrode with an expected change of $\Delta C \approx 400$ fF. These explanations have been confirmed with visual recordings made by an optical microscope camera. In addition, the C_0-V_{bias} shows an asymmetric response due to possible charges trapped inside a thin unetched dielectric layer or inside the substrate. These also affect the non-ideal behavior where sharp transitions are expected. The inspected membranes (7x devices) show resonance frequencies in the 29.15 – 127 kHz range, above the audible range (f > 20 kHz) at $P = 10^{-4}$ kPa. The physical parameters associated with the solution of a harmonic oscillator can be extracted from Eq. 4.

$$f_{01} = \frac{1}{2\pi}\sqrt{\frac{k_{01}}{m_{01}}} = \frac{2.405}{2\pi R}\sqrt{\frac{n_0}{\rho t}} \qquad (4)$$

For the fundamental mode, the $k_i = 4.8967 \cdot n_0$ is the modal stiffness, n_0 the pre-tension, the $m_i = 0.2695 \cdot m$ is the modal mass, $m = \rho t \pi R^2$ is the total mass, ρ the mass density of the graphene and t the membrane thickness. Considering $t = 7$ nm, $\rho = 2267$ kg/m^3, R = 320, 220 µm, without involving any additional masses from possible polymer residuals due to photoresist coating for the lift-off step, the calculated pre-tension for the three geometries are 0.002 N/m (geom. A), 0.02 N/m (Geom. B) and 0.0015 N/m (Geom. C). The fully clamped geometry is stiffer than the trampoline structures in line with the previous $V_{pull\text{-}in}$ tests. An example of f_{01} for a fully clamped drum with 2R = 220 µm is shown in Fig. 6. The reported results refer to measurements performed in low pressure ($P = 10^{-4}$ kPa) to minimize any damping, air loading, and squeeze film effects that might compromise the f_{01} position with partial shifting. Figure 7

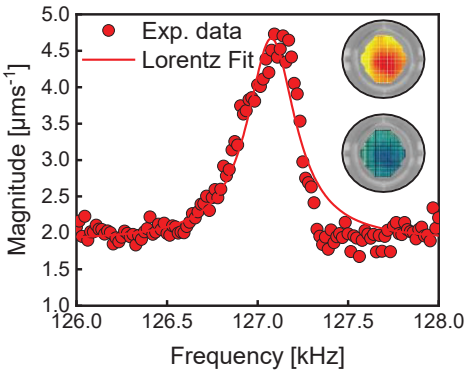

Figure 6: Resonance frequency (1st mode) of ML-gr fully clamped with 2R=220 µm is detected with Polytec MSA-400. A visualization of the described mode is shown as insight.

shows a benchmark of the most recent works on using graphene in a capacitive architecture. This work shows one of the highest aspect ratios reported for devices based on only graphene, where no polymers are involved. Finally, an estimation of the sensitivity of the fabricated devices is calculated by Eq. 5.

$$S = \frac{V_{bias}\, C_m}{gap} \qquad (5)$$

Based on the obtained experimental results, with a minimum V_{bias} = 1.5 V, a gap = 5 µm, and a C_m = 10 – 100 nm/Pa at 1 kHz (from previous work [9]), an estimated S = 3 – 30 mV/Pa is obtained, compared to the S = 5 – 17.8 mV/Pa of the state-of-the-art of MEMS microphones.

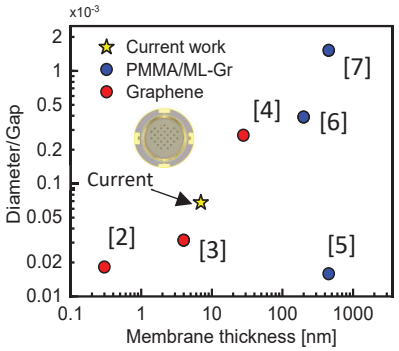

Figure 7: Benchmark of graphene on cavities aspect ratios. This paper, as addition, shows a 100 mm wafer micro machining fabrication flow with integrated patterned electrodes suitable for future System In-Packages demonstrator.

CONCLUSIONS

We demonstrated a wafer-scale transfer-free process to realize multi-layer graphene condenser microphones with a high aspect-ratio for future sensitive miniaturized MEMS devices. With pull-in voltages up to 9.5 V and resonance frequency limited bandwidths of up to 127 kHz. The work opens up an efficient way to realize next-generation graphene microphones with a 4.5x area reduction and an estimated sensitivity of up to 30 mV/Pa.

ACKNOWLEDGEMENTS

The authors thank the Delft University of Technology Else Kooi Lab staff for processing support. This project has received funding from Union's Horizon 2020 research and innovation program under Grant Agreement No. 881603 (Graphene Flagship).

REFERENCES

[1] M. Fueldner, Chapter 48 – Microphones, Handbook of Silicon Based MEMS Materials and Technologies (Third Edition), Elsevier, 2020, pp.937-948.

[2] S. Wittmann, C. Glacer, S. Wagner, S. Pindll, Max C. Lemme, "Graphene Membranes for Hall Sensors and Microphones Integrated with CMOS-Compatible Processes", ACS Applied Nano Materials, 2, 8, pp. 5079– 5085, 2019.

[3] A.F. Carvalho, A. J.S. Fernandes, M. B. Hassine, P. Ferreira, E. Fortunato, F. M. Costa, "Millimeter-sized few-layer suspended graphene membranes", Applied Materials Today, vol. 21, 100879, 2020.

[4] D. Todorović, A. Matković, M. Milićevic, D. Jovanović, R. Gajić, I. Salom, M. Spasenović, "Multi-layer graphene condenser microphone", 2D Materials, et al., 2D Materials, 2, 045013, 2015.

[5] J. Xu, G. S. Wood, E. Mastropaolo, M. J. Newton, R. Cheung, "Realization of Closed Cavity Resonator Formed by Graphene-PMMA Membrane for Sensing Audio Frequency", IEEE Sensors Journal, vol. 20, pp. 4618-4627, 2020.

[6] G. S. Wood, A. Torin, A. K. Al-mashaal, L. S. Smith, E. Mastropaolo, M.J. Newton, R. Cheung, "Design and Characterization of a Micro-Fabricated Graphene-Based MEMS Microphone", IEEE Sensors Journal, vol. 19, pp. 7234 – 7242, 2019.

[7] J. Xu, G. S. Wood, E. Mastropaolo, M. J. Newton, R. Cheung, "Realization of a Graphene/PMMA Acoustic Capacitive Sensor Released by Silicon Dioxide Sacrificial Layer", ACS Applied Materials & Interfaces, 13, 32, pp. 38792-38798, 2021.

[8] G. Baglioni, R. Pezone, S. Vollebregt, K. C. Zobenica, M. Spasenović, D. Todorović, H. Liu, G. J. Verbiest, H. S. J. van der Zant, P.G. Steeneken, "Ultra-sensitive graphene membranes for microphone applications", Nanoscale, 2023.

[9] R. Pezone, G. Baglioni, P.M. Sarro, P.G. Steeneken, S. Vollebregt, "Sensitive Transfer-Free Wafer-Scale Graphene Microphones", ACS Applied Materials & Interfaces, 18, 18, 21705-21712, 2022.

[10] D. R. Lenski, M. S. Fuhrer, "Raman and optical characterization of multi-layer turbostratic graphene grown via chemical vapor deposition", Journal of Applied Physics, vol. 110, 013720, 2011.

[11] I. O. Wygant, M. Kupnik, B. T. Khuri-Yakub, "An Analytical Model for Capacitive Pressure Transducers With Circular Geometry", Journal of Microelectromechanical Systems, vol. 27, pp. 448 – 456, 2018.

CONTACT

*R.P. , tel: +31-(0)15-2786788; r.pezone@tudelft.nl.